

# RADIOSENSOR DIAGNOSTICS OF HIGH-VOLTAGE CIRCUITS

DOI: 10.36724/2072-8735-2025-19-10-61-67

**Manuscript received** 20 July 2025;  
**Accepted** 28 September 2025

**Konstantin A. Boikov,**  
 RTU MIREA, Moscow, Russia, [nauchnyi@yandex.ru](mailto:nauchnyi@yandex.ru)

**Sergey M. Pechenkin,**  
 RTU MIREA, Moscow, Russia, [spechenkin1999@mail.ru](mailto:spechenkin1999@mail.ru)

**Keywords:** radio-sensor diagnostics, high-voltage circuits, phase regulation, signal radio profile, triac, contactless debugging, pulse switching

This paper explores the potential of radio sensor diagnostics for contactless debugging and monitoring of high-voltage electronic circuits where traditional contact measurements are either technically impossible or result in significant distortions in the electronic component's operation. The object of this study is a phase control circuit for an AC induction motor. The primary objective of this work is to improve the debugging efficiency of high-voltage circuits by developing and experimentally verifying a method for diagnosing switching processes and identifying parametric deviations in control circuits based on signal radio profile analysis. The methodology includes recording parasitic electromagnetic radiation, its spectral-temporal processing using a windowed Fourier transform, decomposing the signal radio profile into elementary emitters, and establishing quantitative relationships between their parameters (resonant frequency, attenuation coefficient, initial amplitude, and onset time) and the circuit's operating modes. Analytical relationships are obtained between the amplitude of the initial oscillations of the signal radio profile components, the phase control angle, and the motor's power consumption. The ability to determine the triggering moment of a triac, diagnose opto-isolator degradation, snubber circuit faults, and control pulse generation failures was experimentally confirmed. Requirements for the sensitivity of the measuring equipment and diagnostic conditions were established. It was demonstrated that, when these conditions are met, radio-sensor diagnostics ensures high safety and non-destructive testing without interfering with the circuit's operation. The results can be used in the design, debugging, and maintenance of high-voltage converter devices, especially in conditions that prevent electrical contact with the equipment under test.

## Information about authors:

**Konstantin A. Boikov,** Doctor of Engineering Sciences, Professor, Department of Radio Wave Processes and Technologies, Institute of Radio Electronics and Informatics, RTU MIREA, Moscow, Russia, ORCID 0000-0003-0213-7337

**Sergey M. Pechenkin,** postgraduate student, assistant professor, Department of Radio Wave Processes and Technologies, Institute of Radio Electronics and Informatics, RTU MIREA, Moscow, Russia, ORCID 0009-0000-9360-9082

## Для цитирования:

Бойков К.А., Печенкин С.М. Радиосенсорная диагностика высоковольтных цепей // Т-Комм: Телекоммуникации и транспорт. 2025. Том 19. №10. С. 61-67.

## For citation:

K.A. Boikov, S.M. Pechenkin, "Radiosensor diagnostics of high-voltage circuits," *T-Comm*, 2025, vol. 19, no. 10, pp. 61-67.

## Introduction

Modern high-voltage electronic devices, from household power controllers and dimmers to industrial frequency converters, uninterruptible power supplies, and electric drive control systems, increasingly utilize semiconductor switches such as triacs, thyristors, and IGBT transistors to efficiently and precisely control electrical energy flows [1-3]. These components provide high switching speed, low losses, and digital control capabilities, making them indispensable in modern power electronics. However, these very advantages create significant challenges during circuit debugging and diagnostics.

Directly connecting measuring equipment, particularly an oscilloscope, to circuits live at line voltage (220 V, 380 V, and higher) carries the risk of equipment damage and operator safety. To ensure galvanic isolation, specialized equipment must be used: voltage or current measuring transformers [4, 5], high-voltage differential probes, optical isolation sensors, or isolated oscilloscope inputs. Unfortunately, all of these solutions have significant limitations, resulting in distortion of the measured signal, as well as the introduction of phase shifts, bandwidth limitations (often down to several megahertz), and the introduction of time delays and nonlinearities. Such distortions are especially critical when analyzing high-speed switching processes, where the accuracy of determining the moment of switch on or off directly impacts the assessment of losses, electromagnetic compatibility, and the reliability of the entire system.

It should be noted that despite these limitations, the contact measurement method retains certain advantages. In particular, it allows the use of widely available portable oscilloscopes [6] with a relatively low sampling rate (units to tens of megahertz), since key switching timing parameters, such as the voltage zero crossing point or the duration of the control pulse, can be detected without ultra-high-speed recording. However, such simplified diagnostics become insufficient when developing precision control systems, which require analyzing high-frequency parasitic oscillations caused by parasitic inductances and capacitances on printed circuit boards, as well as assessing current and voltage dynamics in the nanosecond range. This creates a need for alternative diagnostic methods capable of providing high time and frequency resolution without interfering with the circuit under test, without risking the operator or measuring equipment.

## Problem statement and research methods

Under the above conditions, the use of contactless diagnostic methods is particularly relevant. They do not require an electrical connection to the test object and, as a result, eliminate the risk of damaging measuring equipment, compromising signal integrity, or introducing parasitic loads into the circuit under study. Such methods preserve the circuit's natural operating mode, which is critical when analyzing high-speed transients sensitive to the slightest impedance changes.

One promising approach in this area is radio sensor diagnostics (RSD), a method based on recording the inherent parasitic electromagnetic radiation generated by rapid changes in currents and voltages in printed circuit board conductors, power switches, and parasitic elements (mounting inductances, interelectrode capacitances, parasitic resonant circuits). This radiation contains information about the time, frequency, and energy characteristics of

switching events and can be recorded using a broadband receiving antenna and a high-speed digital oscilloscope [7-10]. The RSD offers a number of fundamental advantages, providing complete galvanic isolation between the test object and the measuring instrument. At the same time, when assessing the temporal and spectral parameters of transient processes, the RSD enables the localization of radiation sources based on temporal and frequency characteristics. Moreover, since the radiation is generated by the circuit itself during its operation, the RSD does not require the introduction of external test signals or design modifications.

The goal of this work is to improve the efficiency of debugging and monitoring high-voltage electronic circuits through the systematic use of the RSD as a universal, non-destructive, and safe diagnostic tool.

An illustrative example of the application of the RSD for diagnostics and debugging of high-voltage equipment is the phase control circuit of an AC induction motor (Fig. 1), typical for many industrial and domestic applications.

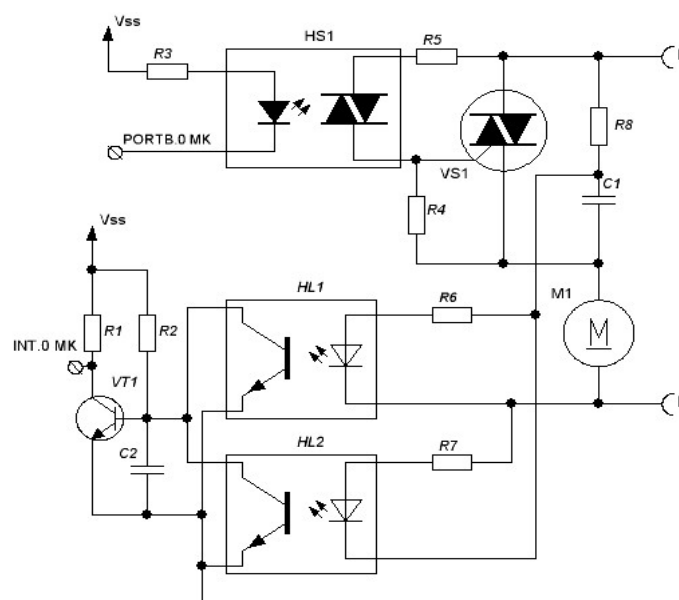


Fig. 1. Phase control circuit of an AC motor

In the circuit under consideration, the power of a single-phase asynchronous motor *M1*, connected to a 220 V AC network via terminals *L* (phase) and *N* (neutral), is controlled by a triac *VS1*. The triac is controlled via an opto-triac isolator *HS1*, the output of which is connected to the control electrode of triac *VS1*. The trigger signal is generated by an *MK ATmega16* microcontroller (not shown in the circuit) on the *PORTB.0* line.

To synchronize control actions with the phase of the network voltage, a zero-crossing detection circuit [11] is implemented. This function is implemented using opto-isolators *HL1* and *HL2* and an inverting stage on transistor *VT1*. Capacitor *C2* acts as a low-pass filter to bypass high-frequency interference, preventing spurious switching of *VT1*. The detector output signal is fed to the microcontroller's external interrupt input (*INT0*), ensuring precise timing of control intervals to the line voltage zero-crossing moments.

At a line frequency of 50 Hz, the voltage period is 20 ms. Thus, when the detection circuit is operating correctly, an interrupt is

generated at 10 ms intervals, corresponding to each half-period of the line voltage.

The firing angle  $\alpha$  (phase cutoff angle), which determines the effective power supplied to the motor, is set programmatically by the microcontroller relative to the line voltage zero-crossing moment, enabling phase control within each half-period of the supply voltage. [12].

When switching the *VSI* triac, sharp dynamic transients occur in the power circuit current and voltage surges, accompanied by the generation of broadband pulsed electromagnetic radiation in the frequency range from a few megahertz to several gigahertz. This radiation, known as the signal radio profile (SRP), carries information about the timing of the semiconductor switch on and off, the amplitude of the switching current, the presence of parasitic resonances caused by the printed circuit board topology, and the parametric deviations of the circuit components. The SRP is recorded in the near field (5–10 cm) using a log-periodic ultra-wideband antenna (e.g., HE 400 UWB, 0.3–6 GHz), a low-noise amplifier, and a high-speed oscilloscope with a sampling rate of  $\geq 10$  GSa/s [13]. The block diagram of the measuring setup is shown in Fig. 2.

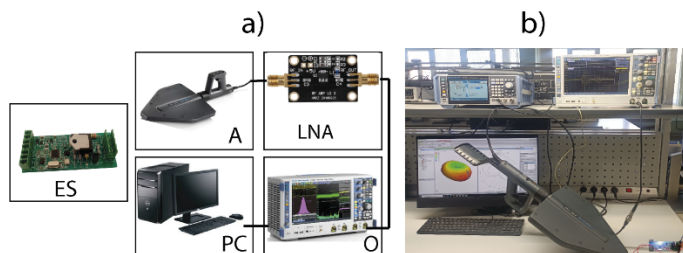


Fig. 2. Measuring stand: a – block diagram; b – photo

A – HE400UWB 0.3 – 6 GHz ultra-wideband measuring antenna (Germany);

LNA – 10M-8 GHz low-noise ultra-wideband amplifier (China);

O – RTO2032 ultra-high-speed real-time oscilloscope (Germany);

PC – personal computer with SRP analysis software;

ES – experimental test sample of the 11ME136-1000W motor phase-control board (China).

This measuring setup demonstrates how SRP analysis allows one to identify triac triggering moments, assess the state of optocouplers, diagnose snubber circuit faults, and correlate the amplitude-frequency parameters of the radiation with the control angle and power consumption.

Thus, in this paper, SRP is positioned not as an auxiliary, but as the primary diagnostic methodology for modern high-voltage converter devices, especially in conditions where contact methods are unacceptable or insufficiently informative.

It was previously shown that the SRP  $U(t)$  can be analytically represented as a superposition of free damped oscillations  $U_{CBi}(t)$  [14, 15]:

$$U(t) = \sum_{i=1}^N U_{CBi}(t) = \sum_{i=1}^N U_{0i} e^{-\delta_i(t-t_{0i})} \sin[\omega_i(t-t_{0i})], \quad (1)$$

where  $U_0$  is the initial amplitude of oscillations,  $\delta$  is the attenuation coefficient,  $\omega$  is the angular frequency of oscillations,  $t$  is the current moment in time,  $t_0$  is the moment in time of the beginning of the emission of the  $i$ -th oscillation.

It should be noted that the initial amplitude of oscillations is proportional to the rate of increase of current  $I$  and, consequently, to the power level [16]:

$$U_{0i}(t) \propto \left. \frac{dI}{dt} \right|_{t=t_{0i}} \quad (2)$$

Thus, even without direct access to the high-voltage circuit, it is possible to evaluate both the time (1) and energy (2) parameters of the high-voltage circuit operation.

In each half-period of the mains voltage, at the moment  $t_{0i} = \alpha/\omega$ , the triac opens, causing a sharp surge in current and the generation SRP. Recording the SRP allows not only to accurately determine the triac firing time, corresponding to  $t_{0i}$ , but also to estimate the power consumed by the motor, identifying firing angle instability. The RSD provides a direct, non-invasive, and highly accurate assessment of switching events, whereas using a measuring transformer during contact diagnostics distorts the signal shape, inverts the phase, and smooths out transient processes, making it impossible to accurately determine  $t_{0i}$ .

### Phase shift problem with inductive loads

When controlling a purely resistive load, such as a heating element, the current and voltage are in phase, and the moment of activation of the *VSI* triac uniquely determines the current waveform and power consumption. However, with an inductive load, typical of motor windings, the current lags the voltage by an angle of  $\varphi = \arctan(\omega_c L_c / R_c)$ , where  $\omega_c$  is the angular frequency of the network,  $L_c$  is the winding inductance, and  $R_c$  is the active resistance.

Due to this phase shift between the current and voltage, *VSI* remains open until the load current drops below the holding current level. With an inductive load, the current crosses zero with a delay relative to the voltage, creating conditions for so-called  $dv/dt$  turn-on, i.e., spontaneous activation of the triac at the beginning of the next half-period even in the absence of a control pulse [17].

At small delay angles  $\alpha$ , the current may not have time to reach sufficient amplitude before its natural zero crossing, leading to asymmetry in the current waveform in the positive and negative half-cycles. The use of current transformers to record these processes introduces additional phase error due to the dynamic characteristics of the measuring circuits.

Furthermore, most phase-shift control systems are synchronized based on the line voltage zero crossing, while the actual switching moment is determined by the dynamics of the load current. This discrepancy between the specified  $\alpha$  angle and the actual moment of energy transfer leads to a systematic control error and a decrease in the accuracy of output power regulation.

The RSD method overcomes these problems, as it responds directly to switching events, rather than to voltage or current separately. If a second pulse appears in the SRP during a half-cycle without a corresponding control signal, this is a clear indication of false triac triggering due to high  $dv/dt$  [18]. RSD allows for the detection of this effect non-contactingly and without distortion, unlike contact methods, where parasitic capacitance and inductance of probes can mask or simulate such phenomena.

With an inductive load, fluctuations in the turn-on moment are possible due to temperature drift, component aging, or changes in the load on the motor shaft. RSD allows for recording the SRP

over multiple periods and generating statistics based on  $t_{0i}$ . Deviations from the reference distribution (e.g., an increase in  $t_{0i}$  variance) indicate degradation of the control circuit.

### Methodology for conducting RSD and obtained results

For the correct application of RSD to high-voltage circuits, it is necessary to meet a number of conditions, as outlined in [13]:

1. Position the antenna in the zone of maximum radiation.
2. Use measuring equipment with a bandwidth of at least 0.3-5 GHz and a sampling rate of at least 10 GSa/s.
3. Conduct measurements in a shielded environment or with low RF background.
4. The signal-to-noise ratio must be at least 17 dB; otherwise, the reliability of the SRP decomposition drops sharply.

Fig. 3 shows SRPs taken at different triac firing angles, i.e., at different motor power levels, while meeting the above conditions.

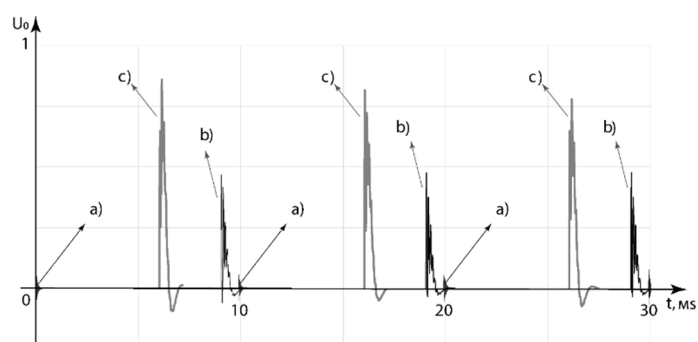


Fig. 3. SRP: a) interrupt block; b) triggering the triac at  $\alpha = 30^\circ$ ; c) triggering the triac at  $\alpha = 60^\circ$

Fig. 3a shows the interrupt block's SRP generated using optical isolators *HL1*, *HL2*, and switching transistor *VTI*, designed to detect the line voltage's zero-crossing moments and generate the corresponding control pulses. It can be seen that the SRP generation period is 10 ms, which corresponds to the duration of a half-period of line voltage at a frequency of 50 Hz and confirms the correct operation of the interrupt signal generation circuit.

For a quantitative analysis of the spectral-temporal characteristics of the interrupt block's signal, a frequency-time transform was used, followed by SRP decomposition and correlation verification of the extracted spectral components [19, 20] (Table 1).

Table 1

Interrupt Block SRP Parameters

Emitters	$N$	$f$ , GHz	$\delta$ , ns <sup>-1</sup>	$t_0$ , ns	$U_0$
1	2	0,50	-0,13	0	0,03
2		0,51	-0,10	7,0	0,02

As can be seen from Table 1, two dominant emitters corresponding to physical processes in the circuit have been identified: the first is caused by disturbances during transistor optocoupler turn-on, and the second by switching of output transistor *VTI*. The closeness of the resonant frequencies is explained by the dominant influence of filter capacitance *C2* on the parasitic oscillatory circuit. The  $U_0$  amplitudes are normalized relative to the maximum SRP response recorded with standard phase control. Using the SRP of a functioning device as a reference allows us to establish reference parameters and identify deviations indicating possible

faults, in particular, degradation of the optical isolation or output inverter.

Fig. 3b and 3c show the SRPs recorded during triac activation at control angles of  $\alpha = 30^\circ$  and  $\alpha = 60^\circ$ , respectively. The parameters of the adopted SRPs are listed in Tables 2 and 3.

Table 2

Parameters of the SRP at  $\alpha = 30^\circ$

Emitters	$N$	$f$ , GHz	$\delta$ , ns <sup>-1</sup>	$t_0$ , ns	$U_0$
1	2	0,10	-0,41	0	0,49
2		0,02	-1,30	0	0,18

Table 3

Parameters of the SRP at  $\alpha = 60^\circ$

Emitters	$N$	$f$ , GHz	$\delta$ , ns <sup>-1</sup>	$t_0$ , ns	$U_0$
1	2	0,10	-0,41	0	0,84
2		0,02	-1,30	0	0,30

Analysis shows that in both cases, the switching transients are formed by two dominant emitters. The first is caused by the current pulse applied to the load, and the second by the dynamics of the snubber circuit. Both emitters occur almost simultaneously ( $t_0 = 0$ ), indicating their common causal relationship with the switching moment.

A clear dependence of the initial amplitude of the main emitter  $U_0$  on the control angle is observed: as  $\alpha$  increases from  $30^\circ$  to  $60^\circ$ , the normalized amplitude increases from 0.49 to 0.84. This is explained by the increase in the instantaneous line voltage at the moment of switching, which leads to an increase in the switching transient energy. The attenuation parameters  $\delta$  and resonant frequencies  $f$  remain unchanged, since they are determined exclusively by the passive components of the circuit – the parasitic inductances and capacitances of the printed circuit board, the snubber parameters, and the load.

As with the chopper block, using the SRP of a functioning device as a reference allows us to determine reference values of spectral parameters and identify anomalies indicating potential faults such as triac degradation, insufficient snubber circuit efficiency, or control pulse generation failure. Furthermore, decomposing the SRP at different control angles allows us to quantitatively study the dependence of the initial amplitude  $U_0$  on the switching phase, as shown in Fig. 4. This approach enables a systematic assessment of the impact of phase control on the energy and timing parameters of the output signal.

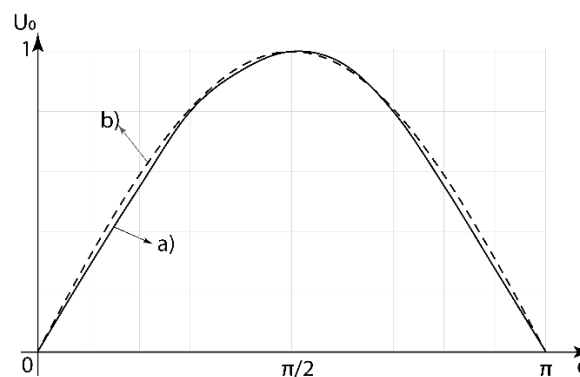


Fig. 4. Dependence of the initial amplitude of the SRP on the control angle: a – real SRP, b – approximation

An analysis of the SRP shown in Fig. 4a shows that the initial oscillation amplitude is approximated by a shape close to a half-wave sine wave (Fig. 4b). This is explained by the harmonic nature of the line voltage and current, which, in the ideal case, are described by a sine function with a frequency of 50 Hz.

Considering that the maximum initial SRP amplitude is achieved at a triac firing angle of  $\alpha = \pi/2$ , the dependence of the initial amplitude  $U_{0i}$  on the control angle  $\alpha$  can be approximated by the following expression:

$$U_{0i}(\alpha) \approx U_{0max} \sin(\alpha), 0 \leq \alpha \leq \pi \quad (3)$$

where  $U_{0max}$  is the amplitude of the SRP at  $\alpha = \pi/2$ .

Fig. 5 shows the experimentally measured dependence of the active power consumed by the motor, recorded by a digital wattmeter, on the triac firing angle  $\alpha$ . The resulting characteristic reflects the effect of phase control on the load's energy parameters.

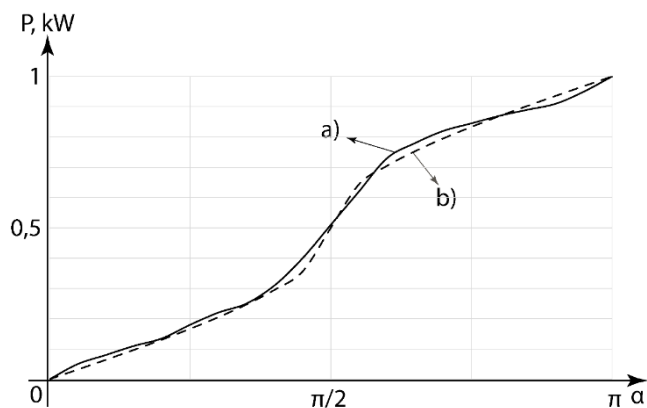


Fig. 5. Engine power versus ignition angle: a – measurements, b – approximation

Analysis of the experimental data presented in Fig. 5a shows that the dependence of the active power  $P(\alpha)$  consumed by the motor on the firing angle of the triac  $\alpha$  can be approximated by a linear function (Fig. 5b):

$$P(\alpha) \approx P_{max} \left( 1 - \frac{\alpha}{\pi} \right), 0 \leq \alpha \leq \pi \quad (4)$$

where  $P_{max}$  is the maximum motor power

Taking into account the previously obtained approximation of the initial amplitude of the SRP  $U_0$  (3) and taking into account that the  $\sin(\alpha)$  function becomes invertible when dividing the interval  $[0, \pi]$  into two regions  $[0, \pi/2]$  and  $(\pi/2, \pi]$ , it is possible to express the motor power as a function of the measured initial amplitude of the SRP  $U_{0i}$  and the known half-period of switching on. Taking into account (4), the dependence of the motor power on the initial amplitude of the SRP can be written as:

$$P(U_{0i}, \alpha) \approx \begin{cases} 1 - \frac{\arcsin(U_{0i})}{\pi}, & \alpha \leq \frac{\pi}{2} \\ \frac{\arcsin(U_{0i})}{\pi}, & \alpha > \frac{\pi}{2} \end{cases} \quad (5)$$

Expression (5) enables non-invasive estimation of the instantaneous active power consumed by the motor based on an analysis of the adopted power supply schedule, subject to calibration using the maximum amplitude  $U_{0max}$  and determination of the half-period of operation. This approach opens the possibility of implementing non-destructive methods for monitoring the load's energy parameters in phase-controlled power control systems.

## Conclusion

Radio sensor diagnostics is a highly effective, completely non-destructive method for examining and continuously monitoring high-voltage electronic systems. As demonstrated in the paper, its key advantage is that it does not require physical connection of measuring sensors to live circuits. This is especially important in cases where traditional contact measurement methods are either fundamentally impossible (for example, due to lack of access to test points or galvanic isolation requirements) or inevitably disrupt the normal operation of the device. Indeed, connecting even high-impedance probes can introduce parasitic capacitance, inductance, or leakage, which distort signal waveforms, alter switching timing, or even trigger abnormal conditions such as false tripping or overvoltage.

The effectiveness of radio sensor diagnostics is clearly demonstrated using the example of a phase control system for an AC induction motor, widely used in industrial and household power controllers. In such a system, correct operation directly depends on the precise synchronization of control pulses with the moment the line voltage crosses zero. Using the RSD, it becomes possible to contactlessly and in real time evaluate critical parameters: the functional integrity of the zero-crossing detection unit, i.e., confirmation that the circuit correctly detects the moments of supply voltage polarity reversal and the actual moment of power-switching element activation, which directly determines the control angle and, consequently, the power transmitted to the load.

The SRP emitted by the device during switching allows not only to visualize these events but also to quantify their temporal relationships. Based on empirical dependencies linking the amplitude, width, and repeatability of characteristic pulses in the SRP with the electrical parameters of the circuit, approximate estimates of the active power consumed by the load can also be obtained. Although this assessment does not claim metrological accuracy, it proves extremely useful for operational monitoring of energy consumption and the identification of anomalies or degradation trends.

The high versatility of the RSD method is due to the fact that virtually any power electronic system, during switching, generates unique electromagnetic "fingerprints" reflecting its internal state. This allows the RSD to be successfully applied in a wide variety of applications:

1. In pulsed power supplies, the method enables the diagnosis of overvoltage and resonant surges based on the appearance of additional high-frequency spectral components in the SRP profile that are absent during normal operation. Breakdowns in power switches, open transformer or inductor windings, and other catastrophic failures manifest themselves as a sharp change, weakening, or complete disappearance of characteristic spectral peaks in the SRP profile, enabling fast and reliable diagnostics without disassembling the device.

2. In inverter converters (e.g., in variable-frequency drives or solar inverters), the RSD can be used to monitor phase switching symmetry, which is critical for current balance and minimizing harmonic distortion. Furthermore, analyzing the time intervals between successive pulses in the SRS allows one to indirectly estimate the duration of the "dead time," the pause between turning off the upper switch and turning on the lower switch in a half-bridge cell, which is necessary to prevent shoot-through currents.

The use of the SRP is particularly valuable for the early detection of gate driver degradation. Over time, due to component aging, thermal cycling, or partial damage to the control lines, the time stamp of the start of the control pulse  $t_{oi}$  can gradually shift. Such microsecond changes are generally imperceptible with conventional oscilloscope monitoring, but are clearly recorded in the phase structure of the SRP, allowing for the prediction of failure before it occurs.

It is important to emphasize that the full potential of the SRP can only be realized if certain requirements for measuring equipment and diagnostic conditions are met. In particular, the receiving path must have sufficient sensitivity to detect weak emissions, an adequate bandwidth covering the characteristic frequencies of switching processes, and control of the electromagnetic environment in the measurement zone to minimize the influence of external interference.

When these conditions are met, the RSD method ensures not only the restoration of key time and energy parameters of the device's operation, but also complete preservation of electrical safety for both the operator and the equipment being diagnosed. Moreover, since diagnostics are performed remotely and passively, they can be carried out in continuous monitoring mode in real time, without the need to stop the process, open the housing, or otherwise interfere with the system's operation. This makes RSD is particularly attractive for use in critical, continuously running or hard to reach power and industrial installations.

### References

- [1] A.P. Evdokimov, A.A. Leshchenko, "Triac power regulator with digital control," *Innovative technologies in the agro-industrial complex in the context of digital transformation: Proceedings of the International scientific and practical conference*, Volgograd, February 9-11, 2022. Vol. II. Volgograd: Volgograd State Agrarian University. 2022, pp. 24-31.
- [2] T.M. Khalina, M.I. Stalnaya, S.Yu. Eremochkin, D.V. Dorokhov, "Reversible adjustable semiconductor bridge three-phase triac rectifier," *Bulletin of the Altai State Agrarian University*. 2021. No. 3, pp. 113-119.
- [3] V.I. Smirnov, A.A. Gavrikov, V.F. Neychev, "Modulation Method for Measuring Thermal Resistances in Power Modules on IGBT Transistors," *News of Higher Educational Institutions. Electronics*. 2025. Vol. 30, No. 1, pp. 40-50. DOI 10.24151/1561-5405-2025-30-1-40-50.
- [4] V.S. Polyakov, A.A. Pugachev, "Requirements for Antiresonant Voltage Transformers," *Electric Power. Transmission and Distribution*. 2023. No. 1, pp. 108-113.
- [5] D.Yu. Pisarev, A.V. Bukreev, "Development and manufacture of an electrical circuit for a soft start system for an electronic converter," *Electrical technologies and electrical equipment in the agro-industrial complex*. 2025. Vol. 72, No. 2, pp. 53-59. DOI 10.22314/2658-4859-2025-72-2-53-59.
- [6] K.A. Volobuev, V.M. Moskaleva, I.V. Trubin, V.G. Trubin, "Power supply of the SDS1102 oscilloscope from the network and an external battery," *Bulletin of Tomsk Polytechnic University. Industrial cybernetics*. 2025. Vol. 3, No. 1, pp. 1-7. DOI 10.18799/29495407/2025/1/81.
- [7] M.S. Kostin, K.A. Boikov, "Digital technologies of signal radio vision and radio monitoring," *Russian Technological Journal*, 2024. Vol. 12. No. 1, pp. 59-69. <https://doi.org/10.32362/2500-316X-2024-12-4-59-69>.
- [8] K.A. Boikov, "Development and study of a radio pulse regeneration system for high-speed stroboscopic digitization devices," *Journal of Radio Electronics [electronic journal]*, 2018. No. 3. Access mode: <http://jre.cplire.ru/jre/mar18/6/text.pdf/> Access date: 26.09.2025.
- [9] K.A. Boikov, "Stages of radiosensor technical diagnostics of electronic devices," *Devices*. 2023. No. 8, pp. 1-7.
- [10] M.S. Kostin, K.A. Boikov, "Cyclogenerative systems for high-speed digitization of non-stationary subnanosecond processes," *Journal of Radio Electronics [electronic journal]*, 2017. No. 6. Access mode: <http://jre.cplire.ru/jre/jun17/8/text.pdf>. Access date: 09.26.2025.
- [11] S.A. Podobuev, E.A. Budkina, A.A. Krylovich, "Development and study of methods for reducing the methodological error of frequency measurement for the signal zero-crossing method," *South Siberian Scientific Bulletin*. 2024. No. 6, pp. 44-56. DOI 10.25699/SSSB.2024.58.6.055.
- [12] D.M. Shishov, D.A. Shevtsov, D.V. Sukhov, "Sensorless Electric Motor Controller with Amplitude-Frequency-Phase Control," *Materials Science. Power Engineering*. 2020. Vol. 26, No. 4, pp. 112-122. DOI 10.18721/JEST.26409.
- [13] K.A. Boikov, "Fault Localization Using Radiosensor Diagnostics," *Elektrosvyaz*. 2023. No. 8, pp. 38-43. DOI: 10.34832/ELSV.2023.45.8.004
- [14] K.A. Boikov, "Modeling and Analysis of Oscillatory Energy Redistribution during Intrinsic Electromagnetic Radiation in Key Electronic Circuits Based on MOSFETs," *Journal of Radio Electronics [electronic journal]*, 2021. No. 6. DOI <https://doi.org/10.30898/1684-1719.2021.6.14>
- [15] K.A. Boikov, "Radiosensor Identification and Authentication of Radioelectronic Devices," *T-Comm*. 2022. Vol. 16. No. 5, pp. 15-20.
- [16] A.I. Korshunov, "Digital System for Maintaining Optimal Power Factor of Active-Inductive Load," *Practical Power Electronics*. 2024. No. 4, pp. 6-11.
- [17] T.M. Khalina, M.I. Stalnaya, S.Yu. Eremochkin, D.V. Dorokhov, "Reversible Adjustable Semiconductor Bridge Three-Phase Triac Rectifier," *Bulletin of the Altai State Agrarian University*. 2021. No. 3, pp. 113-119.
- [18] I. Almpanis, P. Evans, M. Antoniou, "10kV+ Rated SiC n-IGBTs: Novel Collector-Side Design Approach Breaking the Trade-Off between  $dV/dt$  and Device Efficiency," *Key Engineering Materials*. 2023. Vol. 946, pp. 125-133. DOI 10.4028/p-21h51t.
- [19] K.A. Boikov, "Determination of Electronic Device Parameters by Passive Radiosensor Technical Diagnostics," *News of Higher Educational Institutions of Russia. Radio Electronics*. 2021. Vol. 24. No. 6, pp. 63-70.
- [20] M.S. Kostin, K.A. Boikov, "Cyclogenerative systems for actuated digitization of subnanosecond radio pulses in radio vision," *Engineering Physics*, 2018. No. 1, pp. 41-47.

## РАДИОСЕНСОРНАЯ ДИАГНОСТИКА ВЫСОКОВОЛЬТНЫХ ЦЕПЕЙ

**Бойков Константин Анатольевич**, РТУ МИРЭА, Россия, Москва, ORCID 0000-0003-0213-7337, [nauchnyi@yandex.ru](mailto:nauchnyi@yandex.ru)  
**Печенкин Сергей Михайлович**, РТУ МИРЭА, Россия, Москва, ORCID 0009-0000-9360-9082, [spechenkin1999@mail.ru](mailto:spechenkin1999@mail.ru)

**Аннотация**

В данной работе исследуются возможности радиосенсорной диагностики для бесконтактной отладки и мониторинга высоковольтных электронных цепей, где традиционные контактные измерения технически невозможны или приводят к существенным искажениям в работе электронного компонента. Объектом исследования является схема фазового управления асинхронным двигателем переменного тока. Основной целью работы является повышение эффективности отладки высоковольтных цепей путем разработки и экспериментальной проверки метода диагностики коммутационных процессов и выявления параметрических отклонений в цепях управления на основе анализа радиопрофиля сигнала. Методология включает регистрацию паразитного электромагнитного излучения, его спектрально-временную обработку с использованием оконного преобразования Фурье, разложение радиопрофиля сигнала на элементарные излучатели и установление количественных связей между их параметрами (резонансной частотой, коэффициентом затухания, начальной амплитудой и временем установления) и режимами работы схемы. Получены аналитические зависимости между амплитудой начальных колебаний компонент радиопрофиля сигнала, углом фазового управления и потребляемой двигателем мощностью. Установлены требования к чувствительности измерительной аппаратуры и условиям диагностирования. Показано, что при соблюдении этих условий радиосенсорная диагностика обеспечивает высокую безопасность и неразрушающий контроль без нарушения работы схемы. Результаты могут быть использованы при проектировании, отладке и обслуживании высоковольтных преобразовательных устройств, особенно в условиях, исключающих электрический контакт с контролируемым оборудованием.

**Ключевые слова:** радиосенсорная диагностика, высоковольтные цепи, фазовая регулировка, радиопрофиль сигнала, бесконтактная отладка, импульсная коммутация

**Литература**

1. Евдокимов А.П., Лещенко А.А. Симисторный регулятор мощности с цифровым управлением // Инновационные технологии в АПК в условиях цифровой трансформации: Материалы Международной научно-практической конференции, Волгоград, 9-11 февраля 2022 г. Том II. Волгоград: Волгоградский ГАУ. 2022. С. 24-31.
2. Халина Т.М., Стальная М.И., Еремочкин С.Ю., Дорохов Д.В. Реверсивный регулируемый полупроводниковый мостовой трехфазный симисторный выпрямитель // Вестник Алтайского ГАУ. 2021. № 3. С. 113-119.
3. Смирнов В.И., Гавриков А.А., Нейчев В.Ф. Модуляционный метод измерения тепловых сопротивлений силовых модулей на IGBT-транзисторах // Известия высших учебных заведений. Электроника. 2025. Т. 30, № 1. С. 40-50. DOI 10.24151/1561-5405-2025-30-1-40-50.
4. Поляков В.С., Пугачев А.А. Требования к антирезонансным трансформаторам напряжения // Электроэнергия. Передача и распределение. 2023. № 1. С. 108-113.
5. Писарев Д.Ю., Букреев А.В. Разработка и изготовление электрической схемы системы плавного пуска электронного преобразователя // Электротехнологии и электрооборудование в АПК. 2025. Т. 72, № 2. С. 53-59. DOI 10.22314/2658-4859-2025-72-2-53-59.
6. Волобуев К.А., Москалева В.М., Трубин И.В., Трубин В.Г. Питание осциллографа SDS1102 от сети и внешнего аккумулятора // Известия Томского политехнического университета. Промышленная кибернетика. 2025. Т. 3, № 1. С. 1-7. DOI 10.18799/29495407/2025/1/81.
7. Костин М.С., Бойков К.А. Цифровые технологии сигнального радиовидения и радиоконтроля. Российский технологический журнал. 2024. Т. 12. № 1. С. 59-69. <https://doi.org/10.32362/2500-316X-2024-12-4-59-69>.
8. Бойков К.А. Разработка и исследование системы регенерации радиоимпульсов для высокоскоростных стробоскопических устройств оцифровки // Журнал "Радиоэлектроника" [электронный журнал], 2018. № 3. Режим доступа: <http://jre.cplire.ru/jre/mar18/6/text.pdf>/ Дата обращения: 26.09.2025.
9. Бойков К.А. Этапы радиосенсорной технической диагностики электронных устройств // Приборы. 2023. № 8. С. 1-7.
10. Костин М.С., Бойков К.А. Циклогенерационные системы для высокоскоростной оцифровки нестационарных субнаносекундных процессов. // Радиоэлектроника [электронный журнал], 2017. № 6. Режим доступа: <http://jre.cplire.ru/jre/jun17/8/text.pdf>. Дата доступа: 26.09.2025.
11. Подобуев С.А., Будкина Е.А., Крылович А.А. Разработка и исследование методов снижения методической погрешности измерения частоты для метода пересечения сигнала через ноль // Южно-Сибирский научный вестник. 2024. № 6. С. 44-56. DOI 10.25699/SSSB.2024.58.6.055.
12. Шишов Д.М., Шевцов Д.А., Сухов Д.В. Бездатчиковый регулятор электродвигателя с амплитудно-частотно-фазовым управлением // Материаловедение. Энергетика. 2020. Т. 2. № 3. С. 255-256. 26, № 4. С. 112-122. DOI 10.18721/JEST.26409.
13. Бойков К.А. Локализация неисправностей с использованием радиосенсорной диагностики // Электросвязь. 2023. № 8. С. 38-43. DOI: 10.34832/ELSV.2023.45.8.004
14. Бойков К.А. Моделирование и анализ колебательного перераспределения энергии при собственном электромагнитном излучении в ключевых электронных схемах на основе МОП-транзисторов. Радиоэлектроника [электронный журнал], 2021. № 6. DOI <https://doi.org/10.30898/1684-1719.2021.6.14>
15. Бойков К.А. Радиосенсорная идентификация и аутентификация радиоэлектронных устройств // T-Comm: Телекоммуникации и транспорт. 2022. Т. 16. № 5. С. 15-20.
16. Коршунов А.И. Цифровая система поддержания оптимального коэффициента мощности активно-индуктивной нагрузки // Практическая силовая электроника. 2024. № 4. С. 6-11.
17. Халина Т.М., Стальная М.И., Еремочкин С.Ю., Дорохов Д.В. Реверсивный регулируемый полупроводниковый мостовой трёхфазный симисторный выпрямитель // Известия Алтайского государственного аграрного университета. 2021. № 3. С. 113-119.
18. Almpanis I., Evans P., Antoniou M. 10kV+ Rated SiC n-IGBTs: Novel Collector-Side Design Approach Breaking the Compromise Between dV/dt and Device Efficiency // Ключевые инженерные материалы. 2023. Т. 946. С. 125-133. DOI 10.4028/p-21h5lt.
19. Бойков К.А. Определение параметров электронных устройств методом пассивной радиосенсорной технической диагностики // Известия высших учебных заведений России. Радиоэлектроника. 2021. Т. 24. № 6. С. 63-70.
20. Костин М.С., Бойков К.А. Циклогенерационные системы для управляемой оцифровки субнаносекундных радиоимпульсов в радиовидении. // Инженерная физика, 2018. № 1. С. 41-47.